ELSEVIER

International Journal of Mass Spectrometry 198 (2000) 83–96

International Journal of Mass Spectrometry

Opportunities for optimization of the rf signal applied to electrodes of quadrupole mass spectrometers. Part I. General theory

Ernst P. Sheretov

Department of Physics, Ryazan State Radio Technical University, 391000 Ryazan, Russia

Received 11 August 1999; accepted 3 January 2000

Abstract

In this article we define the basic requirements for rf waveform optimization based on the general theory of charged particle trapping for quadrupole mass spectrometers. To satisfy these requirements we introduce and describe a new type of a signal called the EC signal. Also discussed are the features of harmonic and rectangular EC signals. (Int J Mass Spectrom 198 (2000) 83–96) © 2000 Elsevier Science B.V.

Keywords: Mass spectrometry; Mass filter; Hill equation; Ion trap mass spectrometry

1. Introduction

From the early days of quadrupole mass spectrometer (QMS) development it has been clear that the performance of this instrument could be dramatically improved by the appropriate rf waveform selection. Initially, researchers concentrated their efforts on applying rf voltage with a simple rectangular waveform to quadrupole mass filters and ion traps [1,2]. Interest in this trend has been fueled by opportunities for substantial modification of the general stability zone configuration and structure, which would yield important improvements in the performance of mass spectrometers. For example, it has been shown in [3] that sensitivity of the ion trap can be increased by a factor of 4–5 by changing the pulse period-to-pulse duration ratio up to 5. One of the practical realizations of this idea was the three-dimensional ion trap driven by a pulse rf voltage that was developed for the VEGA space program (Venus and Haley's Comet exploration program) [4]. As indicated by the work of Kiai et al. [5, 6], parameters of the ion trap can be improved by modifying a waveform of the rf voltage. Moreover, the use of advanced digital technology and modern computer capabilities allows for dynamic generation of an arbitrary rf waveform during mass scanning.

However, the full potential of this technique has yet to be realized, because so far, no general approach toward the rf waveform optimization problem has been developed. This was due to lack of a general theory of charged particle trapping for the fields, in which the ion motion is described by the Hill equation. Only with the development of such theory will there be an opportunity for optimization of rf voltage applied to electrodes of QMS. The base trapping

E-mail: sheretov@eac.ryazan.su

PII S1387-3806(00)00165-2

theory of "stable" and "unstable" particles for particular cases of the Hill equation [sinewave (the Mathieu equation) and rectangular rf waveform] was described in [7–12] for a sinewave rf waveform, and, for instance, in [13] for a rectangular rf waveform.

In the first part of this work an attempt is made to develop general principles of the trapping theory for QMS without committing to a particular rf waveform. From this theory we obtain a general equation that determines the maximal amplitude of ion oscillation within such devices. By using the Hill equation properties we obtain the equations that determine the size of the trapping area along coordinate axes (in the coordinate space) in the general form. The dimensions of the trapping area were considered parameters for determining the sensitivity of an instrument. This allowed us to define optimization criteria for the shape of the rf potential applied to QMS electrodes. Based of the obtained requirements for rf waveforms we introduce a new rf waveform that we call the EC signal. The features of the two EC signal types (harmonic and rectangular) are later discussed.

2. Amplitude of charged particle oscillations

In order to develop the general theory of ion trapping in the case when we omit the practical effects of the ion–neutral and ion–ion collisions, driving voltage instability, and nonlinear fields in the QMS, we can use the Hill equation.

Let us consider the Hill equation that describes ion trajectories within the QMS (linear mode) in the following form:

$$\ddot{y}(t) + \psi(t)y(t) = 0 \tag{1}$$

where $\psi(t)$ is a periodic function of period T_0. The solution of Eq. (1) can be written in the form [14]

$$y(t) = y_0 Y_1(t_0, t) + \dot{y}_0 Y_2(t_0, t) \tag{2}$$

where

$$Y_1(t_0, t) = \frac{1}{\gamma_0}\left[\dot{y}_2(t_0)y_1(t) - \dot{y}_1(t_0)y_2(t)\right] \tag{3}$$

$$Y_2(t_0, t) = \frac{1}{\gamma_0}\left[y_1(t_0)y_2(t) - y_2(t_0)y_1(t)\right] \tag{4}$$

where γ_0 is the Wronskian determinant; $y_1(t)$ and $y_2(t)$ are two particular independent solutions of Eq. (1); t_0 is the initial phase; and y_0, $\dot{y}_0$ are the initial coordinate and velocity (for $t = t_0$).

Particular independent solutions satisfy the transformation equation

$$\begin{vmatrix} y_1(t + T_0) \\ y_2(t + T_0) \end{vmatrix} = \begin{vmatrix} \alpha_1\alpha_2 \\ \beta_1\beta_2 \end{vmatrix} \times \begin{vmatrix} y_1(t) \\ y_2(t) \end{vmatrix} \tag{5}$$

where α_1 and α_2, β_1 and β_2 are elements of the transformation matrix of partial solutions [14].

The general solutions of Eq. (1) fulfill to the following recursion [14]:

$$y(t + T_0) + y(t - T_0) = 2\beta y(t) \tag{6}$$

where β is the stability parameter of Eq. (1); $2\beta = \alpha_1 + \beta_2$.

First introduced in [1], the characteristic solution of Eq. (1) satisfies Eq. (6) for any values of coefficients A_0 and B_0:

$$y_{\text{character}}(n) = A_0 \cos \nu n T_0 + B_0 \sin \nu n T_0 \tag{7}$$

where $\cos \nu T_0 = \beta$, and n is the time of flight in periods of T_0.

If we find the respective values of coefficients A_0 and B_0 from Eqs. (2) and (7), the characteristic solution (7) matches the general solution (2) for the points with period of T_0. These values of A_0 and B_0 can be found by matching Eqs. (2) and (7) for an arbitrary time point t_s (t_s is the moment when the characteristic solution matches the general solution). Then we have

$$\begin{aligned} A_0 &= y_0 Y_1(t_0, t_s) + \dot{y}_0 Y_2(t_0, t_s) \\ B_0 &= \frac{1}{(1 - \beta^2)^{1/2}} \begin{Bmatrix} y_0[Y_1(t_0, t_s + T_0) - Y_1(t_0, t_s)\beta] \\ + \dot{y}_0[Y_2(t_0, t_s + T_0) - Y_2(t_0, t_s)\beta] \end{Bmatrix} \end{aligned} \tag{8}$$

For the amplitude of the characteristic solution we can obtain:

$$Y_m^2 = A_0^2 + B_0^2 \tag{9}$$

Substitution of Eq. (8) into Eq. (9) yields

$$(1 - \beta^2)Y_m^2 = a_0 y_0^2 + 2b_0 y_0 \dot{y}_0 + c_0 \dot{y}_0^2 \tag{10}$$

where

$$a_0 = Y_1^2(t_0, t_s)(1 - \beta^2) + [Y_1(t_0, t_s + T_0) - Y_1(t_0, t_s)\beta]^2 \tag{11}$$

$$b_0 = Y_1(t_0, t_s)Y_2(t_0, t_s)(1 - \beta^2) + [Y_1(t_0, t_s + T_0) - Y_1(t_0, t_s)\beta] \times [Y_2(t_0, t_s + T_0) - Y_2(t_0, t_s)\beta] \tag{12}$$

$$c_0 = Y_2^2(t_0, t_s)(1 - \beta^2) + [Y_2(t_0, t_s + T_0) - Y_2(t_0, t_s)\beta]^2 \tag{13}$$

The value of remainder

$$f = a_0 c_0 - b_0^2 = (1 - \beta^2)[Y_1(t_0, t_s)Y_2(t_0, t_s + T_0) - Y_2(t_0, t_s)Y_1(t_0, t_s + T_0)]^2 \tag{14}$$

is greater than zero. This means that for a fixed Y_m, and for any t_s, T_0, and t_0, Eq. (10) describes an ellipse [for the stable solutions of Eq. (1) $\beta^2 < 1$].

Now, using Eqs. (10), (2), and (5) we can rewrite Eq. (10) in the form

$$Y_m^2 = \frac{F_2(t_s)}{(1 - \beta^2)\gamma_0^2}[y_0^2 F_1(t_0) - y_0 \dot{y}_0 F_3(t_0) + \dot{y}_0^2 F_2(t_0)] \tag{15}$$

where

$$F_1(t_s) = \alpha_2 \dot{y}_2^2(t_s) - \beta_1 \dot{y}_1^2(t_s) + (\alpha_1 - \beta_2)\dot{y}_1(t_s)\dot{y}_2(t_s) \tag{16}$$

$$F_2(t_s) = \alpha_2 y_2^2(t_s) - \beta_1 y_1^2(t_s) + (\alpha_1 - \beta_2) y_1(t_s) y_2(t_s) \tag{17}$$

$$F_3(t_s) = 2\alpha_2 \dot{y}_2(t_s) y_2(t_s) - 2\beta_1 \dot{y}_1(t_s) y_1(t_s) + (\alpha_1 - \beta_2)[\dot{y}_2(t_s) y_1(t_s) + \dot{y}_1(t_s) y_2(t_s)] \tag{18}$$

It should be noted that functions $F_i(t_s)$ in brackets within Eq. (15) depend only on the initial phase t_0 of ion movement, and do not depend on t_s.

It can be shown by a direct substitution that all functions $F_i(t_s)$ are periodic functions of period T_0.

When for a fixed initial phase t_0 in Eq. (15) we change a moment of collating the characteristic solution with the general one, the value of Y_m^2 also changes. If from possible roots t_i of the equation

$$\frac{dF_2(t_s)}{dt_s} = 0 \tag{19}$$

we choose one root t_{0m} for which the value of $F_2(t_{0m})$ is maximal, and insert this value into Eq. (15) instead of $F_2(t_s)$, we obtain an expression for the maximal oscillation amplitude of a stable particle whose trajectory is described by Eq. (1). If we accept $Y_m^2 = 1$ then from Eq. (15) we obtain the equation of an acceptance ellipse in phase space. In general form the equation of such an ellipse is written

$$\frac{(1 - \beta^2)\gamma_0^2}{F_2(t_{0m})} = y_0^2 F_1(t_0) - y_0 \dot{y}_0 F_3(t_0) + \dot{y}_0^2 F_2(t_0) \tag{20}$$

This equation determines trapping conditions for charged particles within quadrupole ion traps along one coordinate depending on injection phase and initial parameters (initial coordinate y_0 and initial velocity $\dot{y}_0$). The trajectory amplitude search technique used here has also been successfully applied to similar problems with the sinewave rf waveform [9].

3. Amplitude-phase characteristic

It can be shown that there are important equations for $F_i(t_s)$:

$$\frac{dF_1(t_s)}{dt_s} = -\psi(t_s)\frac{dF_2(t_s)}{dt_s}, \qquad \frac{dF_2(t_s)}{dt_s} = F_3(t_s) \tag{21}$$

If t_{0i} are the roots of the equation $F_3(t_{0i}) = 0$, then, as follows from Eq. (21), t_{0i} are the extreme

points for $F_1(t_s)$ and $F_2(t_s)$. In this case the functions $F_1(t_0)$ and $F_2(t_0)$ have their extrema for the same initial phases, and t_{0m} is one of the roots t_{0i}. For $F_3(t_{0i}) = 0$ the axes of the acceptance ellipse are positioned along the coordinate axes of the phase plane. Such orientation of the ellipse repeats itself during T_0 as many times as there are roots t_{0i} during the period.

Using the initial conditions of the first ($y_0 = 1$, $\dot{y}_0 = 0$) and second ($y_0 = 0$, $\dot{y}_0 = 1$) kinds and Eq. (15), we can obtain dependencies that are very important for the trapping theory [amplitude-phase characteristics (APC) of the first and second kinds].

APC of the first kind, as follows from Eq. (15), is described by the following expression:

$$Y^2_{m(\text{1st kind})} = \frac{F_2(t_{0m})\,F_1(t_0)}{(1-\beta^2)\gamma_0^2} \tag{22}$$

For APC of the second kind we have

$$Y^2_{m(\text{2nd kind})} = \frac{F_2(t_{0m})\,F_2(t_0)}{(1-\beta^2)\gamma_0^2} \tag{23}$$

We can see from Eq. (21) that $Y^2_{m(\text{1st kind})}$ has extreme points that satisfy the equations

$$\psi(t_{0n}) = 0 \quad \text{or/and} \quad F_3(t_{0i}) = 0 \tag{24}$$

As noted above, t_{0m} is one of the roots t_{0i}. It can be shown by using Eqs. (15) and (21) that for $t_0 = t_{0m}$, $Y^2_{m(\text{1st kind})} = 1$.

The equations shown above are quite general. The fundamental property of APC of the first kind can be described as follows: For any shape of function $\psi(t_s)$ in Eq. (1), and $\dot{y}_0 = 0$, if equation $F_3(t_{0i}) = 0$ has one or more roots, then among them there is an initial phase $t_0 = t_{0m}$ (called optimal phase of the first kind) for which the amplitude of ion excursion remains less than the initial coordinate y_0.

Thus, the optimal phase of the first kind only appears when function $F_3(t_s)$ has one or more zero values during the period. If $F_3(t_s) \neq 0$ during the period T_0, then the APC of the first kind has extrema for $t_0 = t_{0n}$. It should be noted that, as follows from Eq. (23), when $Y^2_{m(\text{1st kind})}$ is minimal for the optimal phase of the first kind, the value of $Y^2_{m(\text{2nd kind})}$ is maximal. The number of extrema of function $Y^2_{m(\text{1st kind})}$ during period T_0 varies throughout the stability diagram. The number of extrema for $t_0 = t_{0n}$ depends on the shape of function $\psi(t_s)$. In the case of a sinewave signal there are only two roots, and they can be found from

$$a - 2q\cos 2t_{0n} = 0 \tag{25}$$

where a and q are the parameters of the Mathieu equation.

In the mode with $a = 0$ these roots are $t_{0n1} = \pi/4$ and $t_{0n2} = 3\pi/4$. In the case of a conventional rectangular waveform, extreme points correspond to signal wavefronts.

Because the function $F_3(t_s)$ may have no zero points at t_{0n}, the APC of the second kind may have fewer extreme values than the APC of the first kind. Thus, the optimal phase of the second kind coincides with the minimum of the APC of the second kind.

The acceptance S_{acc}, which in early publications on quadrupole mass spectrometers theory was considered a measure of sensitivity, can be easily derived from Eq. (15):

$$S_{\text{acc}} = \frac{1}{[\nu_i(t_{0m})]^{1/2}} \tag{26}$$

where $\nu_i(t_{0m})$ is the absolute value of the ratio $F_2(t_{0m})$ to $F_1(t_{0m})$. The value of S_{acc} is independent from the particle injection phase into the rf field.

4. $F_i(t_0)$ for traditional waveforms of the rf potential

In order to define the values of the function $F_i(t_0)$ we must know the forms of partial solutions to the

initial Eq. (1). For instance, if $\psi(t)$ is a harmonic signal, then this equation turns into the Mathieu equation, whose partial solutions are well known [14]:

$$y_1(t) = \sum_{-\infty}^{\infty} C_{2r} \cos(2r + \tilde{\beta})t; \qquad (27)$$

$$y_2(t) = \sum_{-\infty}^{\infty} C_{2r} \sin(2r + \tilde{\beta})t$$

Then we have

$$\alpha_1 = \cos \tilde{\beta}\pi; \qquad \alpha_2 = -\sin \tilde{\beta}\pi;$$

$$\beta_1 = \sin \tilde{\beta}\pi; \qquad \beta_2 = \cos \tilde{\beta}\pi;$$

$$\beta = \cos \tilde{\beta}\pi; \qquad \sin \tilde{\beta}\pi = (1 - \beta^2)^{1/2};$$

$$F_1(t_0) = -\sin \tilde{\beta}\pi[\dot{y}_1^2(t_0) + \dot{y}_2^2(t_0)]$$

$$F_2(t_0) = -\sin \tilde{\beta}\pi[y_1^2(t_0) + y_2^2(t_0)] \qquad (28)$$

$$F_3(t_0) = -2 \sin \tilde{\beta}\pi[\dot{y}_2(t_0)y_2(t_0) + \dot{y}_1(t_0)y_1(t_0)]$$

$$= -2 \sin \tilde{\beta}\pi \sum_{-\infty}^{\infty} \sum_{-\infty}^{\infty} C_{2r}C_{2m}(2m + \tilde{\beta}) \times \sin 2(r - m)t_0$$

The values of t_{0i} can be found from the last equation for the $F_3(t_0)$: $t_{0i1} = 0(\pi)$ and $t_{0i2} = \pi/2$. These values are the phases for extrema of the APC of the first and second kinds.

For $t_0 = t_{0i1} = 0(\pi)$

$$F_1(t_{0i1}) = -(1 - \beta^2)^{1/2}\left(\sum_{-\infty}^{\infty} C_{2r}(2r + \tilde{\beta}) \right)^2 \qquad (29)$$

$$F_2(t_{0i1}) = -(1 - \beta^2)^{1/2}\left(\sum_{-\infty}^{\infty} C_{2r} \right)^2 \qquad (30)$$

For $t_0 = t_{0i2} = \pi/2$

$$F_1(t_{0i2}) = -(1 - \beta^2)^{1/2} \times \left(\sum_{-\infty}^{\infty} C_{2r}(2r + \tilde{\beta})(-1)^r \right)^2 \qquad (31)$$

$$F_2(t_{0i2}) = -(1 - \beta^2)^{1/2}\left(\sum_{-\infty}^{\infty} C_{2r}(-1)^r \right)^2 \qquad (32)$$

Now we see that depending on C_{2r} coefficients, the optimal phase of the first kind corresponds either to t_{0i1} or t_{0i2}. If C_{2r} coefficients do not change their sign, then

$$t_{0m} = 0(\pi) \qquad (33)$$

If the C_{2r} are the alternating quantities, then

$$t_{0m} = \pi/2 \qquad (34)$$

It should be noted that the values of t_{0i} are the roots of equation

$$F_3(t_{0i}) = 0 \qquad (35)$$

There could be other not so obvious roots. In that case functions $F_1(t_0)$ and $F_2(t_0)$ would have more extreme points during the period T_0. Eq. (35) has two roots if the working point is located near the apex of the first stability zone (low values of a and q), and more roots if the working point is located within one of the higher stability zones.

From Eqs. (27) and (26) we can obtain the following expression for the C_{2r} alternating series:

$$S_{\text{acc}} = \left| \frac{\sum_{-\infty}^{\infty} C_{2r}(2r + \tilde{\beta})(-1)^r}{\sum_{-\infty}^{\infty} C_{2r}(-1)^r} \right| \qquad (36)$$

and for the C_{2r} series of a fixed sign:

$$S_{\text{acc}} = \left| \frac{\sum_{-\infty}^{\infty} C_{2r}(2r + \tilde{\beta})}{\sum_{-\infty}^{\infty} C_{2r}} \right| \qquad (37)$$

Then we have

$$\nu_i(t_{0m}) = \left(\frac{\sum_{-\infty}^{\infty} C_{2r}(-1)^r}{\sum_{-\infty}^{\infty} C_{2r}(2r+\tilde{\beta})(-1)^r} \right)^2$$

or (38)

$$= \left[\frac{\sum_{-\infty}^{\infty} C_{2r}}{\sum_{-\infty}^{\infty} C_{2r}(2r+\tilde{\beta})} \right]^2$$

Above, we have shown an example of how the obtained general expressions can be used in the case when Eq. (1) has some particular independent solutions. When it is difficult to find any particular independent solutions, one can consider elements of the transformation matrix for the general solutions of Eq. (1) instead of transformation elements (α_1, α_2, β_1, β_2) introduced above.

If we have

$$\begin{vmatrix} y(t_0+T_0) \\ \dot{y}(t_0+T_0) \end{vmatrix} = \begin{vmatrix} \psi_1(t_0)\psi_2(t_0) \\ \psi_3(t_0)\psi_4(t_0) \end{vmatrix} \times \begin{vmatrix} y_0 \\ \dot{y}_0 \end{vmatrix} \quad (39)$$

then we can obtain the following relationship between $\psi_i(t_0)$ and $F_i(t_0)$:

$$\psi_1(t_0) = \frac{1}{\gamma_0} F_1(t_0)$$

$$\psi_3(t_0) - \psi_2(t_0) = \frac{1}{\gamma_0} F_3(t_0) \quad (40)$$

$$\psi_4(t_0) = -\frac{1}{\gamma_0} F_2(t_0)$$

The following expressions are valid for $\psi_i(t_0)$:

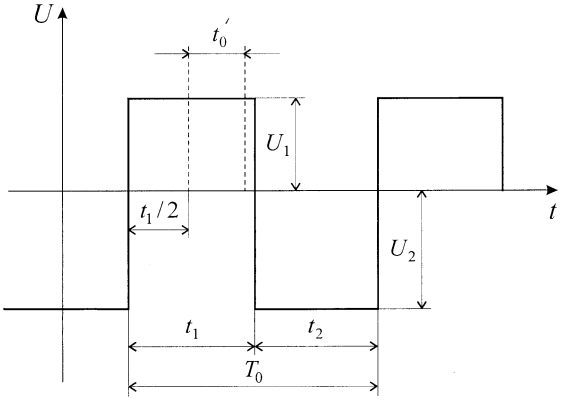

Fig. 1. A conventional rf pulse signal. U_1 and U_2 are the amplitudes of the focusing and defocusing pulses; t_1 and t_2 are the duration of these pulses; t'_0 is a dimensionless quantity ranging from (−0.5) to (+0.5) and measured from the middle of the pulse; T_0 is a period of a pulse signal.

$$2\beta = \psi_2(t_0) + \psi_3(t_0)$$

and (41)

$$\psi_2(t_0)\psi_3(t_0) - \psi_1(t_0)\psi_4(t_0) = 1$$

The introduction of the $\psi_i(t_0)$ functions proved to be an especially effective method of calculating the charged particle trapping conditions when a quadrupole mass spectrometer is driven by a pulse rf voltage (Fig. 1). In this case it is practically impossible to find any partial independent solutions of Eq. (1) due to specific properties of a pulse signal (discontinuity of functions), but it is very easy to define the $\psi_i(t_0)$ functions. It is convenient to use t'_0 instead of t_0.

For a conventional pulse signal such as that shown in Fig. 1 the equation for $\psi_i(t'_0)$ can be written in the form

$$\psi_1(t'_0)_u = a_1 \left\{ \begin{array}{l} \cosh a_2\eta_2 \sinh a_1\eta_1 + \frac{1}{2}\left(\frac{a_1}{a_2} + \frac{a_2}{a_1}\right) \cosh a_1\eta_1 \sinh a_2\eta_2 \\ + \frac{1}{2}\left(\frac{a_2}{a_1} - \frac{a_1}{a_2}\right) \sinh a_2\eta_2 \cosh a_1\eta_1 2t'_0 \end{array} \right\} \quad (42)$$

$$\psi_2(t'_0)_u = \cosh a_2\eta_2 \cosh a_1\eta_1 + \frac{1}{2}\left(\frac{a_1}{a_2}+\frac{a_2}{a_1}\right)\sinh a_2\eta_2 \sinh a_1\eta_1 + \frac{1}{2}\left(\frac{a_1}{a_2}-\frac{a_2}{a_1}\right)\sinh a_2\eta_2 \sinh a_1\eta_1 2t'_0 \quad (43)$$

$$\psi_3(t'_0)_u = \cosh a_2\eta_2 \cosh a_1\eta_1 + \frac{1}{2}\left(\frac{a_1}{a_2}+\frac{a_2}{a_1}\right)\sinh a_2\eta_2 \sinh a_1\eta_1 + \frac{1}{2}\left(\frac{a_2}{a_1}-\frac{a_1}{a_2}\right)\sinh a_2\eta_2 \sinh a_1\eta_1 2t'_0 \quad (44)$$

$$\psi_4(t'_0)_u = \frac{1}{a_1}\left\{\begin{array}{l}\cosh a_2\eta_2 \sinh a_1\eta_1 + \frac{1}{2}\left(\frac{a_1}{a_2}+\frac{a_2}{a_1}\right)\cosh a_1\eta_1 \sinh a_2\eta_2 \\ + \frac{1}{2}\left(\frac{a_1}{a_2}-\frac{a_2}{a_1}\right)\sinh a_2\eta_2 \cosh a_1\eta_1 2t'_0\end{array}\right\} \quad (45)$$

where a_1 and a_2 are coordinates of a working point on the stability diagram

$$a_1^2 = \frac{2\sigma}{1+n_0+p_0}\frac{U_1T_0^2}{z_a^2};$$

$$a_2^2 = \frac{2\sigma}{1+n_0+p_0}\frac{U_2T_0^2}{z_a^2};$$

$$n_0 = \left(\frac{x_a}{z_a}\right)^2; \qquad p_0 = \left(\frac{x_a}{y_a}\right)^2$$

$$\eta_1 = \frac{t_1}{T_0}; \qquad \eta_2 = \frac{t_2}{T_0}$$

where σ is the charge-to-mass ratio; x_a, y_a, and z_a are the closest distances between the centre of the electrode system and the ring and endcap electrodes along the X, Y, and Z axes, respectively; U_1, U_2, t_1, t_2, and T_0 are defined in Fig. 1. The value of t'_0 is a dimensionless quantity ranging from -0.5 to 0.5 and measured from the middle of the pulse.

Eqs. (42)–(45) determine the values of $\psi_i(t'_0)_u$ if t'_0 (initial phase) varies within one pulse [in Eqs. (42)–(45) within the pulse with index 1, Fig. 1]. In order to define the values of $\psi_i(t'_0)_u$ within the pulse with index 2 (Fig. 1), one must swap indices 1 and 2 in the right part of Eqs. (42)–(45). Index u after $\psi_i(t'_0)_u$ shows that these functions represent the pulse signal.

From Eqs. (42)–(45) we see that phase t_{0m} corresponds to $t'_0 = 0$, i.e. the optimal phase of the first kind corresponds to the middle of the pulses (the first or second). Thus, the $\psi_4(t_{0m})$ should be selected from two values defined from the following equations:

$$\psi_{41}(t_{0m}) = \frac{1}{a_1}\left\{\begin{array}{l}\cosh a_2\eta_2 \sinh a_1\eta_1 + \frac{1}{2}\left(\frac{a_1}{a_2}+\frac{a_2}{a_1}\right)\cosh a_1\eta_1 \sinh a_2\eta_2 \\ + \frac{1}{2}\left(\frac{a_1}{a_2}-\frac{a_2}{a_1}\right)\sinh a_2\eta_2\end{array}\right\} \quad (46)$$

and

$$\psi_{42}(t_{0m}) = \frac{1}{a_2}\left\{\begin{array}{l}\cosh a_1\eta_1 \sinh a_2\eta_2 + \frac{1}{2}\left(\frac{a_2}{a_1} + \frac{a_1}{a_2}\right)\cosh a_2\eta_2 \sinh a_1\eta_1 \\ + \frac{1}{2}\left(\frac{a_2}{a_1} - \frac{a_1}{a_2}\right)\sinh a_1\eta_1\end{array}\right\} \quad (47)$$

We should select the maximal value. In Eqs. (46) and (47) if a_1 is an imaginary quantity, then a_2 is a real quantity by definition.

5. Size of the trapping area

As we have mentioned above, it was widely perceived in earlier publications that the area of the acceptance ellipse defines the sensitivity of an instrument, and that sensitivity is proportional to the product of areas of the ellipses for different coordinates. This idea is mainly attractive because the sensitivity is independent from the phase of ion injection into the rf field, which is rather convenient. It also reflects the ability of an instrument to "perceive" ions with high initial coordinates and high initial velocities. However, no one could inject particles into the field in such a manner that the phase space is uniformly filled with ion working points. On the other hand, it follows from experiments that there is a strong dependence between sensitivity and ion injection phase (in some cases this dependence can be attenuated, for example, in the case of 100% transmission for the mass filter).

The current theory of QMS is based on stable particle trapping space. In the ion trap, for example, this is a region where nascent ions can be trapped by the three-dimensional field. The ratio of the trapping space volume to the injection volume of the analyzed particles determines the trapping probability for injected ions and, accordingly, the sensitivity of an instrument. In order to estimate the trapping space volume we should determine trapping areas along coordinate axes. The size of the trapping area for a given coordinate axis can be found from Eq. (10):

$$\Delta_i = 2\delta_i(t_0)(1 - \dot{y}_{0i}^2\nu_i(t_{0m})\delta_i(t_0))^{1/2} \quad (48)$$

where

$$\delta_i(t_0) = \frac{F_1(t_{0m})}{F_1(t_0)} \quad (49)$$

and $\dot{y}_{0i}$ is the projection of the initial velocity on a given axis.

We can see from Eq. (48) that the $\delta_i(t_0)$ function determines the dependency between the trapping area and the initial phase. This function, by definition, has the maximum value for the optimal phase of the first kind. When a phase t_0 is not equal to the optimal phase of the first kind, the value of the $\delta_i(t_0)$ function decreases. The $\delta_i(t_0)$ function has one more (smallest) extremum around the optimal phase of the second kind (from 0.02 to 0.3 depending on rf signal shape and working point location on the stability diagram). The typical shape of the $\delta_i^2(t_0)$ function is shown in Fig. 2. The influence of initial velocities on the trapping area is always negative (i.e. $\dot{y} \neq 0$ always decreases the size of the trapping area and, respectively, the trapping space volume), and depends on the $\nu_i(t_{0m})$ coefficient [see Eq. (26) for the acceptance]. An increase in $\nu_i(t_{0m})$ increases the influence of ion initial velocities and decreases the acceptance.

For initial velocity in Eq. (48) we have

$$\dot{y}_0^2 = \xi_i\Delta_{\text{init}} \quad (50)$$

where $\Delta_{\text{init}} = U_{\text{acc}}/U_{p-p}$; U_{acc} is the accelerating potential difference that determines initial velocity of a particle, U_{p-p} is the rf peak-to-peak voltage applied to electrodes, and ξ_i is a coefficient determined by a rf voltage shape.

In the case of a sinewave signal:

$$\xi_{\text{im}} = 12q \quad (51)$$

For a signal with a rectangular waveform:

$$\xi_{\text{iu}} = 3(a_1^2 + a_2^2) \quad (52)$$

The value of the Δ_{init} coefficient depends on how ions are injected into the working volume of an analyzer.

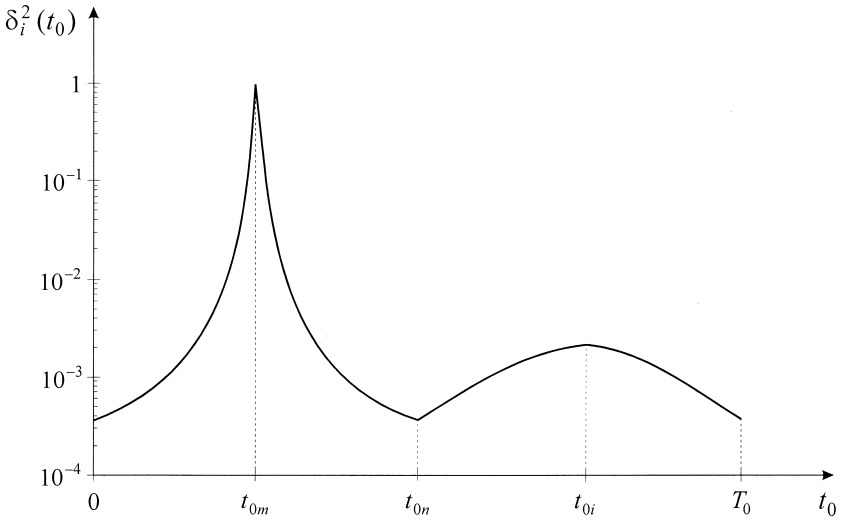

Fig. 2. Variation of $\delta_i^2(t_0)$ as a function of injection phase t_0; t_{0m} is the optimal phase of the first kind; t_{0i} is the optimal phase of the second kind.

When ions are created in the ion trap by electron impact ionization they then have low thermal initial velocities. In this case $U_{acc} \sim \varphi_T = kT/e$, where φ_T is the thermal potential, k is the Boltzmann constant, and e is the electron charge. For $U_{p-p} = 2 \times 10^3$ V the value of Δ_{init} is about 10^{-5}. When ions are injected into the quadrupole mass filter, they have entrance energy of several electron Volts, and their transverse velocities are close to the thermal ones (at best). Under these circumstances we expect an increase in the Δ_{init} value by a factor of 10 and more. The values of $\xi_i \nu_i(t_{0m})$ for the working point located near the upper apex of the stability diagram are presented in Table 1 for the axially symmetric ion trap driven by a harmonic signal and a pulse signal of different ratios λ ($\lambda = t_1/t_2$, see Fig. 1).

A resolution of 190 was found for a given working point on the stability diagram. Working point coordinates are (for a sinewave signal) $a_r = 0.334$, $q_r = 0.619$; $\beta_r = -0.994$, $\beta_z = 0.985$; [for a pulse signal with pulse period-to-pulse duration ratio 2 (meander)] $a_1 = 3.588394$, $a_2 = 2.506333$; $\beta_r = -0.994$, $\beta_z = 0.984$. We can see from Table 1 that the ion trap operates in a high resolution mode, but nevertheless the value of $\dot{y}_{0i}^2 \nu_i(t_{0m})\delta_i(t_0)$ in Eq. (48) is very small. This means that the trapping efficiency (the size of the trapping area) can be described by

$$\Delta_i \cong 2\delta_i(t_0) \tag{53}$$

If the ion trap operates in the mode without a dc potential (for the Mathieu equation $a = 0$), then the value of $\xi_i \nu_i(t_{0m})$ decreases. For a working point with

Table 1
The values of the $\xi_i \nu_i(t_{0m})$ parameter for the axially symmetric ion trap

Harmonic signal	Pulse signal						
	λ						
	6/4	7/3	8/2	1/1	4/6	3/7	2/8
5.1×10^3	3.8×10^3	3.3×10^3	3.1×10^3	4.7×10^3	5.9×10^3	8.2×10^3	1.3×10^4

$a_r = 0$, $q_r = 0.25$, $\tilde{\beta}_r = 0.1790131$, and $\tilde{\beta}_z = 0.3737448$ in the case of a sinewave signal, we obtain for the r coordinate $\xi_i \nu_i(t_{0m}) = 1.6 \times 10^2$. In the case of a rectangular waveform (meander) for $a_1 = a_2 = 1.915$ we obtain $\xi_i \nu_i(t_{0m}) = 1.25 \times 10^2$.

Thus, we can use Eq. (48) for a precise estimation of sensitivity for various operational modes of QMS. However, for further consideration we shall use Eq. (53) for estimation of Δ_i.

For example, let us consider the uniform ionization within the whole working volume of the ion trap during the whole period T_0. The trapping probability in this case can be taken in proportion to the integral P:

$$P = \frac{1}{T_0} \int_0^{T_0} \Delta_x \Delta_y \Delta_z \, dt_0 \tag{54}$$

In practice, however, the restrictions imposed by introduction of integral (54) are often violated. For example, for the ion trap with an electron beam to form ions, an ionization region is commensurable to the trapping region only along one coordinate axis. If the ionizing electron beam is injected along the z axis with low r coordinates, there will be only Δ_z (depending on the phase) under the integral. When the ionizing electron beam is injected through the ring electrode in the radial plane at a right angle to the z axis (in the shape of a wide sheet beam), the ionization region in the z direction is very small. In this case sensitivity is in proportion to the following integral:

$$P = \frac{1}{T_0} \int_0^{T_0} \Delta_x^2 \, dt_0 \tag{55}$$

Because Δ_i is in proportion to $\delta_i(t_0)$, the dependency between Δ_x^2 and t_0 is very close to the dependency in Fig. 2. The value of $\delta_i^2(t_{0m})$ is 10–20 times greater than $\delta_i^2(t_{0i})$ for the points located close to the upper apex of the first stability zone. Thus, integral (55) depends on the $\delta_i^2(t_0)$ function for those values of t_0 that are close to the optimal phase of the first kind, and the range of integration in Eq. (55) can be limited by the phase smaller than t_{0n}. In this case, after replacing the $\delta_i(t_0)$ function with its Taylor approximation around the optimal phase of the first kind, Eq. (55) can be rewritten in the form

$$P = \frac{2(t_{0n} - t_{0m})}{T_0} \left(1 - \sum_{j=1}^{\infty} \frac{(\delta_i^2(t_0))^{(j)}|_{t_0 = t_{0m}}}{j!(j+1)} \times (t_{0n} - t_{0m})^j \right) \tag{56}$$

We see that the maximal sensitivity can be achieved when

$$(\delta_i^2(t_0))^{(i)}|_{t_0 = t_{0m}} = 0 \tag{57}$$

i.e. all derivatives of $\delta_i^2(t_0)$ in the point $t_0 = t_{0m}$ must be sufficiently small or equal to zero. Eq. (57) is a very strong condition. The value of integral (56) can be considerably increased if we can make several first-order derivatives equal to zero. Note that condition (57) can only be fulfilled within some part of the period T_0.

Let us find conditions under which Eq. (57) is fulfilled. From Eqs. (21) and (48) we have

$$\delta_i(t_0) = \frac{F_1(t_{0m})}{F_1(t_0)}; \qquad \frac{dF_1(t_0)}{dt_0} = -\psi(t_0) F_3(t_0) \tag{58}$$

By a successive differentiation of the function $1/F_1(t_0)$ we obtain higher derivatives that are ratios of two functions. The denominator of these ratios includes the $F_1(t_0)$ function of a positive degree. Because $F_1(t_{0m})$ is not equal to zero, the functions in the denominators are nonzero functions for $t_0 = t_{0m}$. The numerator of the higher derivatives includes a sum of functions proportional to $\psi(t_{0m})$, or higher derivatives of $\psi(t_0)$ for $t_0 = t_{0m}$, or proportional to these functions of a positive degree. Eq. (57) is feasible if the following conditions are fulfilled:

$$\psi(t_{0m}) = 0 \qquad \psi^{(i)}(t_0)|_{t_0 = t_{0m}} = 0 \tag{59}$$

In addition to these conditions we should add another condition that follows from Eqs. (2) and (26) that

$$S_{\text{acc}} = \frac{1}{[\nu_i(t_{0m})]^{1/2}} \tag{60}$$

should be maximal.

These are the requirements for the optimal signal $\psi(t)$ in Eq. (1). Meeting these requirements considerably increases the sensitivity of the mass spectrometer.

The first requirement in Eqs. (59), which is the strongest one, is not met for rf signals used at the present time. The second requirement in Eqs. (59) is partially met for a conventional sinewave signal. Here, if we consider the canonical Mathieu equation, $t_{0m} = 0(\pi)$, the first derivative and all odd derivatives of $\psi(t)$ for $t_0 = t_{0m}$ are equal to zero. At the same time, in the case of a pulse signal the second requirement in Eqs. (59) is completely met, whereas the first one is not. From the point of view of the developed theory, a pulse signal is more optimal than a sinewave signal. An rf waveform that satisfies the first condition in Eqs. (59) around the optimal phase of the first kind is called the EC signal.

6. EC signal

A conventional harmonic signal with a dc component can be turned into a harmonic EC signal by superimposing an additional harmonic function. The harmonic EC signal can be expressed in the following form:

$$\psi(t) = a - 2q[\cos 2t + k \cos 2jt] \tag{61}$$

where k should be defined in accordance with the first requirement in Eqs. (59), and j is an integer greater than 1. Having j greater than *3* is possible, but hardly attractive from a practical point of view.

If we assume $j = 2$, then Eq. (61) has three extrema for

$$i_{0_i} = p' \frac{\pi}{2}; \qquad p' = 0, 1, 2, \ldots \tag{62}$$

and two extrema for

$$2t_{0_j} = \arccos(-1) \frac{1}{4k} \tag{63}$$

the optimal phase of the first kind for the r coordinate (for axially symmetric ion trap) corresponds to the focusing field along the radius, i.e. the right part in Eq. (61) must be positive. In order to satisfy this condition we should select $p' = 1$ in Eq. (62). If we assume

$$\psi(t_{01}) = 0 \tag{64}$$

then we obtain the needed value of k:

$$k_{p'=1} = 1 + \frac{a}{2q} \tag{65}$$

From this equation we can see that $k > 1$ and grows with the increasing slope of the scan line. In the mode of operation without a dc potential $a = 0$ and $k = 1$. This mode is very attractive and easy to implement, and this is a simple version of the mass-selective instability mode [15].

The harmonic EC signal ($p' = 1$, $j = 2$, and $a = 0$) is shown in Fig. 3a. A phase $t_{0m} = \pi/2$ in this figure is the optimal phase of the first kind. The signal described by Eq. (61) has all derivatives of odd orders for the optimal phase of the first kind, and $\psi(t_{0m}) = 0$. Otherwise, Eq. (61) meets the requirements in Eqs. (59) only in part, but importantly, the first strong condition is fulfilled.

If in Eq. (61) we assume $j = 3$, then $\psi(t)$ can be written in the form

$$\psi(t) = a - 2q[\cos 2T + k \cos 6T] \tag{66}$$

Here we see that

$$t_{0i} = p'\pi/2 \quad \text{and} \quad p' = 0, 1, 2, \ldots \tag{67}$$

i.e. extrema occupy the same phases.

$$\sin^2 2t_{0j} = \frac{1 + 2k}{12k} \tag{68}$$

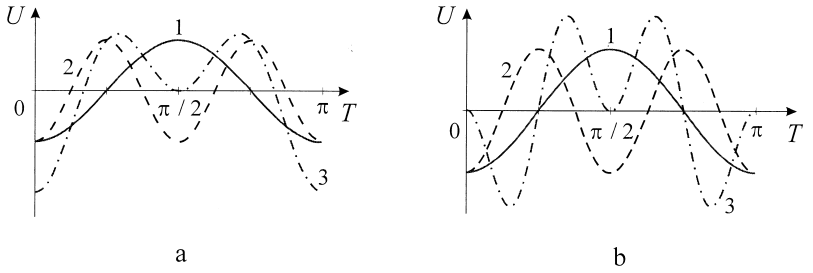

Fig. 3. Harmonic EC signal (one period). (a) Harmonic EC signal with the second harmonic ($p' = 1$, $a = 0$, $j = 2$). Line 1 is the first harmonic, 2 is the second harmonic, and 3 is the harmonic EC signal. (b) Harmonic EC signal with the third harmonic ($p' = 1$, $a = 0$, $j = 3$). Line 1 is the first harmonic, 2 is the third harmonic, and 3 is the harmonic EC signal.

and for k we have the same expression as Eq. (65). The waveform of the harmonic EC signal is shown in Fig. 3b.

Note that the harmonic EC signal that corresponds to $j = 2$ (Fig. 3a) is asymmetric. This means that this signal is optimized along one coordinate axis (the OPC of the first kind for the r coordinate). The signal is not optimized along the z coordinate because the optimal phase of the first kind corresponds to the phase of $0(\pi)$, and the first condition of Eqs. (59) is not fulfilled. The EC signal with $j = 3$ is symmetric (Fig. 3b) and this signal is optimized along both the r and the z coordinates.

In order to meet all the requirements of Eqs. (59), analyzers should be driven by a pulse signal. We have suggested a pulse EC signal [16], the waveform of which is shown in Fig. 4a. Time intervals η_i, which make a period T_0 of the signal, could be set in various proportions. The time interval η_a is called the active part of the EC signal. The active part of the signal shown in Fig. 4a meets the requirements of Eqs. (59) completely for a coordinate axis along which the time interval η_1 is focusing (a force acting upon a charged particle directed toward the origin). The duration of the active part can be set up to a half of the period T_0. Under certain circumstances (shown in Part II) this dramatically increases trapping efficiency and sensitivity of instruments.

A signal shown in Fig. 4 is similar to the harmonic EC signal for $j = 2$. A pulse EC signal having a symmetric structure corresponding to a harmonic EC signal with $j = 3$ is shown in Fig. 4b. The pulse η_1 is focusing (η_2 is defocusing) along one coordinate and defocusing (η_2 is focusing) along the other one. The respective active parts for these pulses are η_{a1} and η_{a2}. It should be noted that the EC signals are easy to generate, especially for the ion trap and monopole mass filter.

In Table 2 we compare the calculated values of $\xi_i \nu_i(t_{0m})$ for a three-dimensional axially symmetric ion trap driven by EC signals. Calculations were carried out for a working point located close to the upper apex of the first stability zone (r coordinate). For the pulse EC signal ($\eta_i = 0.25T_0$) coordinates are $a_1 = 4.40267$, $a_2 = 4.276$; coordinates in the case of the harmonic EC signal ($j = 2$) are $a = 0.471747$, $q = 0.494773$.

The use of the EC signal, as shown in Tables 1 and 2, yields an increase of trapping efficiency for charged particles with nonzero velocities. However, the total increase in sensitivity for QMS can be estimated comparing the integrals of Eq. (55) for driving signals of different waveforms, or by comparison of correctly calculated mass peak shapes, which is more preferable. These issues are addressed in Part II.

Table 2
The values of the $\xi_i \nu_i(t_{0m})$ parameter for the axially symmetric ion trap driven by EC signals

Pulse EC signal	Harmonic EC signal ($j = 2$)
1.1×10^3	2.32×10^3

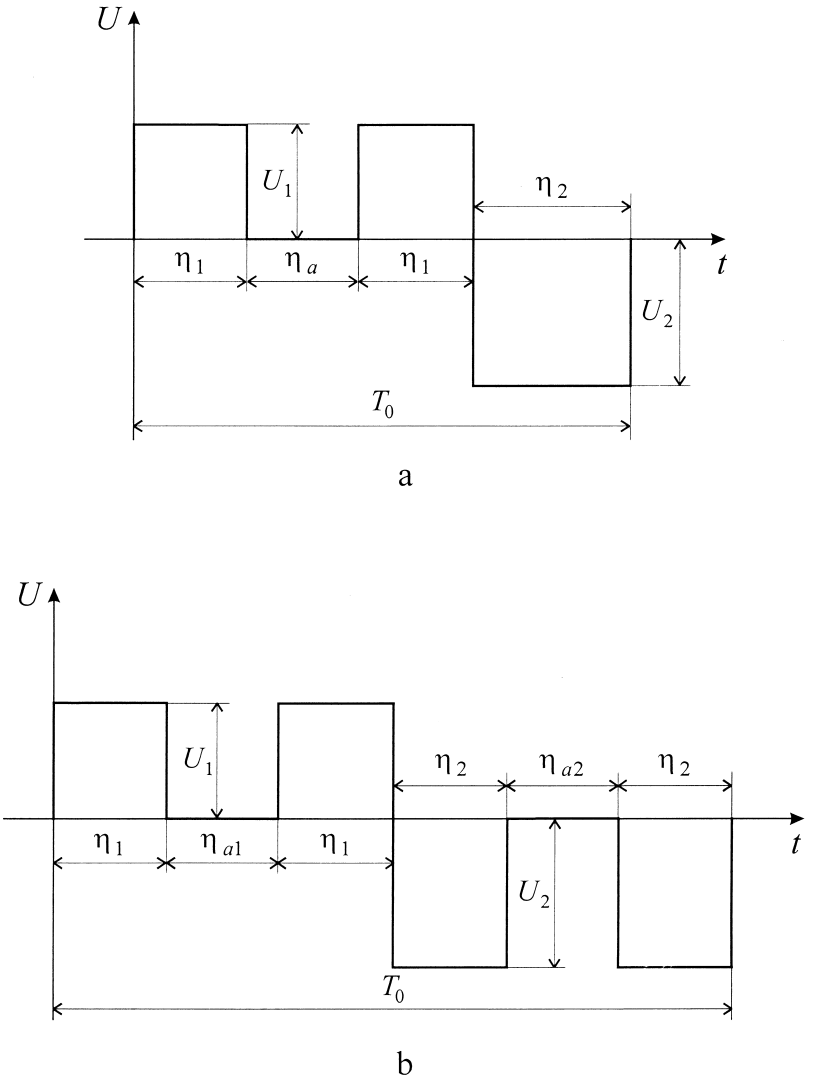

Fig. 4. Pulse EC signal (one period). (a) Asymmetric pulse EC signal (η_a is the active part of the EC signal for the r coordinate); (b) symmetric pulse EC signal (η_{a1} and η_{a2} are the active parts of the EC signal for the r and z coordinates, respectively); U_1 and U_2 are the amplitudes of the focusing and defocusing pulses; η_1 is the relative duration of the focusing pulse and η_2 is the relative duration of the defocusing pulse.

7. Conclusions

This article has (1) demonstrated a general calculation principle for amplitude of ion oscillation within the QMS for an arbitrary periodic waveform; (2) obtained a general expression for the acceptance ellipses and amplitude-phase characteristics of the first and second kinds; (3) obtained a general expression determining the size of the trapping space within the analyzer; (4) formulated and validated requirements for the optimized rf signal applied to electrodes of QMS; (5) suggested the EC signal that completely meets the stated requirements.

Waveforms of both the pulse and harmonic EC signals and their properties have been described.

Acknowledgements

I wish to thank Andrei E. Sheretov and Igor W. Philippov for their assistance in preparing this manuscript. I would like to express my gratitude to the referees for the careful reading of the manuscript and their valuable comments.

References

[1] E.P. Sheretov, W.I. Terent'ev, J. Tech. Phys. 5 (1972) 953.
[2] J.A. Richards, R.M. Huey, J. Hiller, Int. J. Mass Spectrom. Ion Phys. 12 (1973) 317.
[3] N.V. Veselkin, Features of charged particle movement within alternating electrical fields created by hyperboloidal electrode systems, and the development of mass analyzers driven by a pulse signal, Thesis, Ryazan Radio Technical Institute, Ryazan, Russia, 1985.
[4] Y.A. Surkov, F.F. Kirpozov, O.P. Soborcov, V.N. Glazov, A.G. Dunchenko, L.P. Taciy, Astron. J. Lett. 12 (1986) 114.
[5] S.M. Sadat Kiai, J. Andre, Y. Zerega, G. Brincourt, R. Catella, Int. J. Mass Spectrom. Ion Proc. 107 (1991) 191.
[6] S.M. Sadat Kiai, Y. Zerega, G. Brincourt, R. Catella, J. Andre, Int. J. Mass Spectrom. Ion Proc. 108 (1991) 65.
[7] W. Paul, H.R. Reinchard, U. Von Zahn, Z. Phys. 152 (1958) 143.
[8] A.J. Lichtenberg, Phase-Space Dynamics of Particles, Wiley, New York, 1969.
[9] E.P. Sheretov, B.I. Kolotilin, J. Tech. Phys. 42 (1972) 1931.
[10] E.P. Sheretov, B.I. Kolotilin, M.P. Safonov, J. Tech. Phys. 42 (1974) 2604.
[11] R.M. Waldren, J.F.J. Todd, Dyn. Mass Spectrom. 5 (1978) 14.
[12] R.E. March, R.J. Hughes, Quadrupole Storage Mass Spectrometry. 2. VIII, Wiley, New York, 1989, p. 89.
[13] B.I. Kolotilin, A.P. Borisovskiy, W.I. Banin, S.P. Ovtchinnikov, J. Tech. Phys. 58 (1988) 1709.
[14] N.W. McLachlan, Theory and Applications of Mathieu Functions, Clarendon, Oxford, 1947.
[15] G.C. Stafford, P.E. Kelley, J.E.P. Syka, W.R. Reynolds, J.F.J. Todd, Int. J. Mass Spectrom. Ion Processes 60 (1984) 85.
[16] E.P. Sheretov, Power supply technique for hyperboloid mass spectrometers, Russian Patent No. 2068599, 1996.